Application of ensemble transform data assimilation methods for parameter estimation in nonlinear problems

Sangeetika Ruchi[1], Svetlana Dubinkina[1], and Jana de Wiljes[2]

[1]Centrum Wiskunde & Informatica, P.O. Box 94079, 1098 XG Amsterdam, The Netherlands
[2]University of Potsdam, Karl-Liebknecht-Str. 24/25, D-14476, Potsdam, Germany

Correspondence: Jana de Wiljes (wiljes@uni-potsdam.de)

Abstract. Identification of unknown parameters on the basis of partial and noisy data is a challenging task in particular in high dimensional and nonlinear settings. Gaussian approximations to the problem, such as ensemble Kalman inversion, tend to be robust, computationally cheap and often produce astonishingly accurate estimations despite the inherently wrong underlying assumptions. Yet there is a lot of room for improvement specifically regarding the description of the associated statistics. The tempered ensemble transform particle filter is an adaptive sequential Monte Carlo method, where resampling is based on optimal transport mapping. Unlike ensemble Kalman inversion it does not require any assumptions regarding the posterior distribution and hence has shown to provide promising results for non-linear non-Gaussian inverse problems. However, the improved accuracy comes with the price of much higher computational complexity and the method is not as robust as the ensemble Kalman inversion in high dimensional problems. In this work, we add an entropy inspired regularisation factor to the underlying optimal transport problem that allows to considerably reduce the high computational cost via Sinkhorn iterations. Further, the robustness of the method is increased via an ensemble Kalman inversion proposal step before each update of the samples, which is also referred to as hybrid approach. The promising performance of the introduced method is numerically verified by testing it on a steady-state single-phase Darcy flow model with two different permeability configurations. The results are compared to the output of ensemble Kalman inversion, and Markov Chain Monte Carlo methods results are computed as a benchmark.

1 Introduction

If a solution of a considered partial differential equations (PDE) is highly sensitive to its parameters, accurate estimation of the parameters and their uncertainties is essential to obtain a just approximation of the solution. Partial observations of the solution are then used to infer uncertain parameters by solving a PDE-constrained inverse problem. For instance one can approach such problems via methods induced by Bayes's formula (Stuart, 2010). More specifically the posterior probability density of the parameters given the data, is then computed on the basis of a prior probability density and a likelihood which is the conditional probability density associated with the given noisy observations. Well-posedness of an inverse problem and convergence to the true posterior in the limit of observational noise going to zero was proven for different priors and under assumptions on the parameter-to-observation map by Dashti and Stuart (2017), for example.

25   When aiming at practical applications as in oil reservoir management (Lorentzen et al., 2020) and meteorology (Houtekamer and Zhang, 2016) for example, the posterior is approximated by means of a finite set of samples. Markov chain Monte Carlo (MCMC) methods approximate the posterior with a chain of samples–a sequential update of samples according to the posterior. The main drawback of MCMC is that this approach is not parallelizable. Therefore unless a speed up is introduced in a MCMC chain (e.g., Cotter et al., 2013), MCMC is impractical for computationally expensive PDE models.

30   Adaptive Sequential Monte Carlo (SMC) methods, on the contrary, are parallelizable since they approximate the posterior with an *ensemble* of samples by computing their probability (e.g, Vergé et al., 2015). Adaptive intermediate probability measures are introduced between the prior measure and the posterior measure to improve upon method divergence due to the curse of dimensionality following Del Moral et al. (2006); Neal (2001). Moreover, sampling from an invariant Markov kernel with the target intermediate measure and the reference prior measure improves upon ensemble diversity due to parameters

35   stationarity as shown by Beskos et al. (2015). However, when parameter space is high dimensional, adaptive SMC requires computationally prohibitive ensemble sizes unless we approximate only the first two moments (e.g., Iglesias et al., 2018) or we sample highly correlated samples (Ruchi et al., 2019).

     Ensemble Kalman inversion (EKI) approximates only the first two moments of the posterior, which makes it computationally attractive for estimating high dimensional parameters. For linear problems, Blömker et al. (2019) showed well-posedness and

40   convergence of EKI for a fixed ensemble size and without any assumptions of Gaussianity. However for nonlinear problems, Ernst et al. (2015); Evensen (2018) showed that in the large ensemble size limit an EKI approximation is not consistent with the Bayesian approximation.

     In order to sample highly correlated samples, one can employ optimal transport resampling that lies at the heart of the ensemble transform particle filter (ETPF) proposed by Reich (2013). An optimal transport map between two consecutive prob-

45   ability measures provides a direct sample-to-sample map with maximized sample correlation. Along the lines of an adaptive SMC approach a probability measure is described via the importance weights and the deterministic mapping replaces the traditional resampling step. A so-called tempered ensemble transform particle filter (TETPF) was proposed by Ruchi et al. (2019). Note that this ansatz does not require any distributional assumption for the posterior and it was shown by Ruchi et al. (2019) that TETPF provides encouraging results for nonlinear high dimensional PDE-constrained inverse problems. However, the

50   computational cost of solving an optimal transport problem in each iteration is considerably high.

     In this work we address two issues arisen in the context of TETPF: (i) the immense computational costs of solving the associated optimal transport problem and (ii) the lack of robustness of the TETPF with respect to high dimensional problems. More specifically, the performance of ETPF has been found to be highly dependent on the initial guess. Although tempering restrains any sharp fail in the importance sampling step due to a poor initial ensemble selection, the number of required

55   intermediate steps and the efficiency of ETPF still depends on it. Chustagulprom et al. (2016) suggested that the lack of robustness in high dimensions can be addressed via a hybrid approach that combines a Gaussian approximation with the ETPF. Furthermore, Acevedo et al. (2017) suggested that the computational complexity of the ETPF can be significantly reduced via a Sinkhorn approximation to the underlying transport problem. Along the lines of Chustagulprom et al. (2016); de Wiljes

et al. (2020), we propose a tempered ensemble transform particle filter with Sinkhorn approximation (TESPF) and a tempered
hybrid approach.

The remainder of the manuscript is organised as follows: in Sect. 2, the inverse problem setting is presented. There we describe the tempered ensemble transform particle filter (TETPF) proposed by Ruchi et al. (2019). Furthermore, we introduce the
tempered ensemble transform particle filter with Sinkhorn approximation (TESPF), a tempered hybrid approach that combines
EKI and TETPF (hybrid EKI-TETPF), and a tempered hybrid approach that combines EKI and TESPF (hybrid EKI-TESPF).
We discuss computational complexities of all the presented techniques and provide corresponding pseudocodes in Appendix A.
In Sect. 3, we apply the adaptive SMC methods to an inverse problem of inferring high dimensional permeability parameters
for a steady-state single-phase Darcy flow model. Permeability is parameterized following Ruchi et al. (2019), where one
configuration of parametrization leads to Gaussian posteriors, while another one to non-Gaussian posteriors. Finally, we draw
conclusions in Sect. 4.

2 Bayesian inverse problem

We assume $\boldsymbol{u} \in \tilde{\mathcal{U}} \subset \mathbb{R}^n$ is a random variable that is related to partially observable quantities $\boldsymbol{y} \in \mathcal{Y} \subset \mathbb{R}^\kappa$ by a nonlinear
forward operator $F : \tilde{\mathcal{U}} \to \mathcal{Y}$, namely

$$\boldsymbol{y} = F(\boldsymbol{u}).$$

Further $\boldsymbol{y}_{\mathrm{obs}} \in \mathcal{Y}$ denotes a noisy observation of $\boldsymbol{y}$, i.e.,

$$\boldsymbol{y}_{\mathrm{obs}} = \boldsymbol{y} + \boldsymbol{\eta}$$

where $\boldsymbol{\eta} \sim \mathcal{N}(\mathbf{0}, \mathbf{R})$. The aim is to determine or approximate the posterior measure $\mu(\boldsymbol{u})$ conditioned on observations $\boldsymbol{y}_{\mathrm{obs}}$ and
given a prior measure $\mu_0(\boldsymbol{u})$, which is referred to as Bayesian inverse problem. The posterior measure is absolutely continuous
with respect to the prior, i.e.,

$$\frac{\mathrm{d}\mu}{\mathrm{d}\mu_0}(\boldsymbol{u}) \propto g(\boldsymbol{u}; \boldsymbol{y}_{\mathrm{obs}}), \tag{1}$$

where $\propto$ is up to a constant of normalisation and g is referred to as the likelihood and depends on the forward operator F. The
Gaussian observation noise of the observation $\boldsymbol{y}_{\mathrm{obs}}$ implies

$$g(\boldsymbol{u}; \boldsymbol{y}_{\mathrm{obs}}) = \exp\left[-\frac{1}{2}(F(\boldsymbol{u}) - \boldsymbol{y}_{\mathrm{obs}})' \mathbf{R}^{-1}(F(\boldsymbol{u}) - \boldsymbol{y}_{\mathrm{obs}}) \right], \tag{2}$$

where $'$ denotes the transpose.

2.1 Tempered Sequential Monte Carlo

We consider sequential Monte Carlo (SMC) methods that approximate the posterior measure $\mu(\boldsymbol{u})$ via an empirical measure

$$\mu^M(\boldsymbol{u}) = \sum_{i=1}^{M} w_i \delta_{\boldsymbol{u}_i}(\boldsymbol{u}).$$

Here δ is the Dirac function, and the importance weights for the approximation of μ are

$$w_i = \frac{g(\boldsymbol{u}_i; \boldsymbol{y}_{\mathrm{obs}})}{\sum_{j=1}^M g(\boldsymbol{u}_j; \boldsymbol{y}_{\mathrm{obs}})}.$$

An ensemble $\mathcal{U} = \{\boldsymbol{u}_1, \ldots, \boldsymbol{u}_M\} \subset \tilde{\mathcal{U}}$ consists of M realizations $\boldsymbol{u}_i \in \mathbb{R}^n$ of a random variable $\boldsymbol{u}$ that are independent and

90 identically distributed according to $\boldsymbol{u}_i \sim \mu_0$.

When an easy to sample from prior μ_0 does not approximate the complex posterior μ well, only a few weights w_i have significant value resulting in a degenerative approximation of the posterior measure. Potential reasons for this effect are high dimensionality of the uncertain parameter, large number of observations, or accuracy of the observations. An existing solution to a degenerative approximation is an iterative approach based on tempering by Del Moral et al. (2006) or annealing by Neal

95 (2001). The underlying idea is to introduce T intermediate artificial measures $\{\mu_t\}_{t=0}^T$ between μ_0 and $\mu_T = \mu$. These measures are bridged by introducing T tempering parameters $\{\phi_t\}_{t=1}^T$ that satisfy $0 = \phi_0 < \phi_1 < \ldots < \phi_T = 1$. An intermediate measure μ_t is defined as a probability measure that has density proportional to $g(\boldsymbol{u})$ with respect to the previous measure μ_{t-1}

$$\frac{\mathrm{d}\mu_t}{\mathrm{d}\mu_{t-1}}(\boldsymbol{u}) \propto g(\boldsymbol{u}; \boldsymbol{y}_{\mathrm{obs}})^{(\phi_t - \phi_{t-1})}.$$

Along the lines of Iglesias (2016) the tempering parameter ϕ_t is chosen such that effective ensemble size (ESS)

100 $$\mathrm{ESS}_t(\phi) = \frac{\left(\sum_{i=1}^M w_{t,i}\right)^2}{\sum_{i=1}^M w_{t,i}^2}$$

with

$$w_{t,i} = \frac{g(\boldsymbol{u}_{t-1,i}; \boldsymbol{y}_{\mathrm{obs}})^{(\phi_t - \phi_{t-1})}}{\sum_{j=1}^M g(\boldsymbol{u}_{t-1,j}; \boldsymbol{y}_{\mathrm{obs}})^{(\phi_t - \phi_{t-1})}}, \tag{3}$$

does not drop below a certain threshold $1 < M_{\mathrm{thresh}} < M$. Then an approximation of the posterior measure μ_t is

$$\mu_t^M(\boldsymbol{u}) = \sum_{i=1}^M w_{t,i} \delta_{\boldsymbol{u}_{t-1,i}}(\boldsymbol{u}). \tag{4}$$

105 A bisection algorithm on the interval $(\phi_{t-1}, 1]$ is employed to find ϕ. If $\mathrm{ESS}_t > M_{\mathrm{thresh}}$ we set $\phi_t = 1$ which implies that no further tempering is required.

The choice of ESS to define a tempering parameter is supported by results of Beskos et al. (2014) on stability of a tempered SMC method in terms of ESS. Moreover, for a Gaussian probability density approximated by importance sampling, Agapiou et al. (2017) showed that ESS is related to the second moment of the Radon-Nikodym derivative Eq. (1).

110 An SMC method with importance sampling Eq. (4) does not change the sample $\{\boldsymbol{u}_{t-1,i}\}_{i=1}^M$, which leads to the method collapse due to a finite ensemble size. Therefore each tempering iteration t needs to be supplied with resampling. Resampling provides a new ensemble $\{\tilde{\boldsymbol{u}}_{t,i}\}_{i=1}^M$ that approximates the measure μ_t. We will discuss different resampling techniques in Sect. 2.3.

2.2 Mutation

Due to stationarity of the parameters an SMC method requires ensemble perturbation. We use ensemble mutation of Cotter et al. (2013) with the target measure μ_t and the reference measure μ_0. The mutation phase is initialized at $\boldsymbol{v}_{0,i} = \tilde{\boldsymbol{u}}_{t,i}$, and at the final inner iteration $\tau_{\max}$ we assign $\boldsymbol{u}_{t,i} = \boldsymbol{v}_{\tau_{\max},i}$ for $i = 1, \ldots, M$.

For a Gaussian prior we use the preconditioned Crank-Nicolson pcn-MCMC method

$$\boldsymbol{v}_i^{\mathrm{prop}} = \sqrt{1-\theta^2}\,\boldsymbol{v}_{\tau,i} + (1-\sqrt{1-\theta^2})\boldsymbol{m} + \theta\boldsymbol{\xi}_{\tau,i} \quad \text{for} \quad i = 1, \ldots, M. \tag{5}$$

Here $\boldsymbol{m}$ is the mean of the Gaussian prior measure μ_0 and $\{\boldsymbol{\xi}_{\tau,i}\}_{i=1}^M$ are from a Gaussian distribution with zero mean and a covariance matrix of the Gaussian prior measure μ_0.

For a uniform prior $U[a,b]$ we use random walk

$$\boldsymbol{v}_i^{\mathrm{prop}} = \boldsymbol{v}_{\tau,i} + \boldsymbol{\xi}_{\tau,i} \quad i = 1, \ldots, M. \tag{6}$$

Here $\{\boldsymbol{\xi}_{\tau,i}\}_{i=1}^M \sim U[a-b, b-a]$ and $\{\boldsymbol{v}_i^{\mathrm{prop}}\}_{i=1}^M$ are projected onto the $[a,b]$ interval if necessary. Then the ensemble at the inner iteration $\tau+1$ is

$$\boldsymbol{v}_{\tau+1,i} = \boldsymbol{v}_i^{\mathrm{prop}} \quad \text{with the probability} \quad \rho(\boldsymbol{v}_i^{\mathrm{prop}}, \boldsymbol{u}_{t-1,i}) \quad \text{for} \quad i = 1, \ldots, M; \tag{7}$$

$$\boldsymbol{v}_{\tau+1,i} = \boldsymbol{v}_{\tau,i} \quad \text{with the probability} \quad 1 - \rho(\boldsymbol{v}_i^{\mathrm{prop}}, \boldsymbol{u}_{t-1,i}) \quad \text{for} \quad i = 1, \ldots, M. \tag{8}$$

Here $\boldsymbol{v}_i^{\mathrm{prop}}$ is from Eq. (5) for the Gaussian measure and from Eq. (6) for the uniform measure, and

$$\rho(\boldsymbol{v}_i^{\mathrm{prop}}, \boldsymbol{u}_{t-1,i}) = \min\left\{1, \frac{g(\boldsymbol{v}_i^{\mathrm{prop}}; \boldsymbol{y}_{\mathrm{obs}})^{\phi_t}}{g(\boldsymbol{u}_{t-1,i}; \boldsymbol{y}_{\mathrm{obs}})^{\phi_t}}\right\}.$$

The scalar $\theta \in (0, 1]$ controls the performance of the Markov chain. Small values of θ lead to high acceptance rates but poor mixing. Roberts and Rosenthal (2001) showed that for high-dimensional problems it is optimal to choose θ such that the acceptance rate is between 20 % and 30 % by the last tempering iteration T. Cotter et al. (2013) proved that under some assumptions this mutation produces a Markov kernel with an invariant measure μ_t.

Computational complexity. In each tempering iteration t the computational complexity of the pcn-MCMC mutation is $\mathcal{O}(\tau_{\max} M \mathcal{C})$, where $\mathcal{C}$ is computational cost of a forward model F. For the pseudocode of the pcn-MCMC mutation please refer to the Algorithm 1 in Appendix A. Note that the computational complexity is not effected by the length of $\boldsymbol{u}$ which is a very desirable property in high dimensions as shown by Cotter et al. (2013) and Hairer et al. (2014).

2.3 Resampling phase

As we have already mentioned in Sect. 2.1, an adaptive SMC method with importance sampling needs to be supplied with resampling at each tempering iteration t. We consider a resampling method based on optimal transport mapping proposed by Reich (2013).

2.3.1 Optimal transformation

The origin of the optimal transport theory lies in finding an optimal way of redistributing mass which was first formulated by Monge (1781). Given a distribution of matter, e.g., a pile of sand, the underlying question is how to reshape the matter into
145   another form such that the work done is minimal. A century later the original problem was rewritten by Kantorovich (1942) in a statistical framework that allowed to tackle it. Due to these contributions it was later named the Monge-Kantorovich minimization problem.

Let us consider a scenario where the initial distribution of matter is represented by a probability measure μ on the measurable space $\tilde{\mathcal{U}}$, that has to be moved and rearranged according to a given new distribution ν, defined on the measurable space $\tilde{\mathcal{V}}$. Then
150   we seak a probability measure that is a solution to

$$\min\left\{\int_{\tilde{\mathcal{U}}\times\tilde{\mathcal{V}}} c(\boldsymbol{u},\tilde{\boldsymbol{u}})d\omega: \quad \omega\in\prod(\mu,\nu)\right\}, \tag{9}$$

where the minimum is compute over all joint probability measures ω on $\tilde{\mathcal{U}}\times\tilde{\mathcal{V}}$ with marginals μ and ν, and $c(\boldsymbol{u},\tilde{\boldsymbol{u}})$ is a transport cost function on $\tilde{\mathcal{U}}\times\tilde{\mathcal{V}}$. The joint measures achieving the infinum are called optimal transport plans.

Let μ and ν be two measures on a measurable space $(\Omega,\mathcal{F})$ such that μ is the law of random variable $U:\Omega\to\tilde{\mathcal{U}}$ and ν is
155   the law of random variable $V:\Omega\to\tilde{\mathcal{V}}$. Then a coupling of (μ,ν) consists of a pair (U,V). Note that couplings always exist, an example is the trivial coupling in which the random variables U and V are independent. A coupling is called deterministic if there exists a measurable function $\Psi_M:\tilde{\mathcal{U}}\to\tilde{\mathcal{V}}$ such that $V=\Psi_M(U)$ and Ψ_M is called transport map. Unlike general couplings, deterministic couplings do not always exist. On the other hand there may be infinitely many deterministic couplings. One famous variant of Eq. (9), where the optimal coupling is known to be a deterministic coupling, is given by

160
$$\omega^* = \arg\inf_{\omega\in\Pi(\mu,\nu)}\sqrt{\mathbb{E}\|U-V\|^2} \tag{10}$$

where $\Pi(\mu,\nu)$ denotes the set of measures joining μ and ν (see Villani (2008) for details). The aim of the resampling step is to obtain equally probable samples. Therefore, in resampling based on optimal transport of Reich (2013), the Monge-Kantorovich minimization problem Eq. (10) is considered for the current posterior measure $\mu_t^M(\boldsymbol{u})$ given by its samples approximation Eq. (4) and a uniform measure (here the weights in the sample approximation are set to $1/M$). The discretized objective
165   functional of the associate optimal transport problem is given by

$$J(\mathbf{S}) := \sum_{i,j=1}^{M} s_{ij}\|\boldsymbol{u}_{t-1,i}-\boldsymbol{u}_{t-1,j}\|^2$$

subject to $s_{ij}>0$ and constraints

$$\sum_{i=1}^{M} s_{ij}=\frac{1}{M}, \quad j=1,\dots M; \qquad \sum_{j=1}^{M} s_{ij}=w_{t,i}, \quad i=1,\dots M,$$

where matrix $\mathbf{S}$ describes a joint probability measure under the assumption that the state space is finite. Then samples $\{\tilde{\boldsymbol{u}}_{t,i}\}_{i=1}^{M}$ are obtained by a deterministic linear transform, i.e.,

$$\tilde{\boldsymbol{u}}_{t,j} := M \sum_{i=1}^{M} \boldsymbol{u}_{t-1,i} s_{ij} \quad \text{for} \quad j = 1,\ldots,M. \tag{11}$$

Reich (2013) showed weak convergence of the deterministic optimal transformation Eq. (11) to a solution of the Monge-Kantorovich problem Eq. (9) as $M \to \infty$.

Computational complexity. The computational complexity of solving the optimal transport problem with an efficient earth mover distance algorithm such as FastEMD of Pele and Werman (2009) is of order $\mathcal{O}(M^3 \log M)$. Consequently the computational complexity of the adaptive tempering SMC with optimal transport resampling (TETPF) is $\mathcal{O}[T(M\mathcal{C} + M^3 \log M + \tau_{\max} M \mathcal{C})]$, where T is the number of tempering iterations, $\tau_{\max}$ is the number of pcn-MCMC inner iterations, and $\mathcal{C}$ is computational cost of a forward model F. For the pseudocode of the TETPF please refer to the Algorithm 4 in Appendix A.

2.3.2 Sinkhorn approximation

As discussed above solving the optimal transport problem has a computational complexity of $\mathcal{O} = M^3 \log(M)$ in every iteration of the tempering procedure. Thus the TETPF becomes very expensive for large M. One the other hand an increase in the number of samples directly correlates with an improved accuracy of the estimation. In order to allow for as many samples as possible one needs to reduce the associate computational cost of the optimal transport problem. This can be achieved by replacing the optimal transport distance with a Sinkhorn distance and subsequently exploiting the new structure to elude the immense computational time of the EMD solver as shown by Cuturi (2013). More precisely the ansatz is built on the fact that the original transport problem has a natural entropic bound that is obtained for $\mathbf{S} = [\frac{1}{M}\boldsymbol{I}_M \boldsymbol{w}^\top]$ where $\boldsymbol{w} = [w_1,\ldots,w_M]$ and $\boldsymbol{I}_M = [1,\ldots,1] \in \mathbb{R}^M$ which constitutes an independent joint probability. Therefore one can consider the problem of finding a matrix $\mathbf{S} \in \mathbb{R}^{M \times M}$, that is constraint by an additional lower entropic bound (Sinkhorn distance). This additional constraint can be incorporated via a Lagrange multiplier, which leads to the above regularised form, i.e.,

$$J_{\mathrm{SH}}(\mathbf{S}) = \sum_{i,j=1}^{M} \left\{ s_{ij} \|\boldsymbol{u}_{t-1,i} - \boldsymbol{u}_{t-1,j}\|^2 + \frac{1}{\alpha} s_{ij} \log s_{ij} \right\} \tag{12}$$

where $\alpha > 0$. Due to additional smoothness the minimum of Eq. (12) can be unique and has the form

$$\mathbf{S}^\alpha = \mathbf{diag}(\boldsymbol{b}) \exp\left(-\alpha \mathbf{Z}\right) \mathbf{diag}(\boldsymbol{a})$$

where $\mathbf{Z}$ is matrix with entires $z_{ij} = \|\boldsymbol{u}_{t-1,i} - \boldsymbol{u}_{t-1,j}\|^2$ and $\boldsymbol{b}$ and $\boldsymbol{a}$ non-negative vectors determined by employing Sinkhorn's fixpoint iteration described by Sinkhorn (1967). We will refer to this approach as tempered ensemble Sinkhorn particle filter (TESPF).

Computational complexity. Solving this regularise optimal transport problems rather than original transport problem given in Eq. (9) reduces the complexity to $\mathcal{O}(M^2 C(\alpha))$. For the pseudocode of the Sinkhorn adaptation of solving the optimal transport problem please refer to the Algorithm 3 in Appendix A. For the pseudocode of the TESPF please refer to the Algorithm 4 in Appendix A.

2.4 Ensemble Kalman inversion

For Bayesian inverse problems with Gaussian measures, ensemble Kalman inversion (EKI) is one of the widely used algorithm. EKI is an adaptive SMC method that approximates the first two statistical moments of a posterior distribution. For a linear forward model, EKI is optimal in a sense it minimizes the error in the mean (Blömker et al., 2019). For a nonlinear forward model, EKI still provides a good estimation of posterior (e.g., Iglesias et al., 2018). Here we consider EKI method of Iglesias et al. (2018), since it is based on the tempering approach.

The intermediate measures $\{\mu_t\}_{t=0}^T$ are approximated by Gaussian distributed variables with empirical mean $\boldsymbol{m}_t$ and empirical variance $\mathbf{C}_t$. Given empirical mean $\boldsymbol{m}_{t-1}$ and empirical covariance $\mathbf{C}_{t-1}$ defined in terms of $\{\boldsymbol{u}_{t-1,i}\}_{i=1}^M$

$$\boldsymbol{m}_{t-1} = \frac{1}{M}\sum_{i=1}^M \boldsymbol{u}_{t-1,i}, \qquad \mathbf{C}_{t-1} = \frac{1}{M-1}\sum_{i=1}^M (\boldsymbol{u}_{t-1,i}-\boldsymbol{m}_{t-1})\otimes(\boldsymbol{u}_{t-1,i}-\boldsymbol{m}_{t-1}),$$

the mean and covariance are updated by

$$\boldsymbol{m}_t = \boldsymbol{m}_{t-1} + \mathbf{C}_{t-1}^{\mathrm{u\,F}}(\mathbf{C}_{t-1}^{\mathrm{FF}}+\Delta_t\mathbf{R})^{-1}(\boldsymbol{y}_{\mathrm{obs}}-\overline{\boldsymbol{F}}_{t-1}), \qquad \mathbf{C}_t = \mathbf{C}_{t-1} - \mathbf{C}_{t-1}^{\mathrm{u\,F}}(\mathbf{C}_{t-1}^{\mathrm{FF}}+\Delta_t\mathbf{R})^{-1}\mathbf{C}_{t-1}^{\mathrm{uF}}{}',$$

where

$$\mathbf{C}_{t-1}^{\mathrm{uF}} = \frac{1}{M-1}\sum_{i=1}^M (\boldsymbol{u}_{t-1,i}-\boldsymbol{m}_{t-1})\otimes(F(\boldsymbol{u}_{t-1,i})-\overline{\boldsymbol{F}}_{t-1}), \quad \mathbf{C}_{t-1}^{\mathrm{FF}} = \frac{1}{M-1}\sum_{i=1}^M [F(\boldsymbol{u}_{t-1,i})-\overline{\boldsymbol{F}}_{t-1}]\otimes[F(\boldsymbol{u}_{t-1,i})-\overline{\boldsymbol{F}}_{t-1}],$$

$$\Delta_t = \frac{1}{\phi_t-\phi_{t-1}}, \qquad \overline{\boldsymbol{F}}_{t-1} = \frac{1}{M}\sum_{i=1}^M F(\boldsymbol{u}_{t-1,i}).$$

Since we are interested in an ensemble approximation of the posterior distribution, we update the ensemble members by

$$\tilde{\boldsymbol{u}}_{t,i} = \boldsymbol{u}_{t-1,i} + \mathbf{C}_{t-1}^{\mathrm{uF}}(\mathbf{C}_{t-1}^{\mathrm{FF}}+\Delta_t\boldsymbol{R})^{-1}[\boldsymbol{y}_{t,i}-F(\boldsymbol{u}_{t-1,i})] \quad \text{for} \quad i=1,\ldots,M. \tag{13}$$

Here $\boldsymbol{y}_{t,i} = \boldsymbol{y}_{\mathrm{obs}} + \boldsymbol{\eta}_{t,i}$ and $\boldsymbol{\eta}_{t,i} \sim \mathcal{N}(\boldsymbol{0},\Delta_t\mathbf{R})$ for $i=1,\ldots,M$.

Computational complexity. By implementing a sequential observation update of Whitaker et al. (2008), the computational complexity of solving Eq. (13) can be reduced to $\mathcal{O}(2M\kappa n)$, where n is the parameter space dimension, κ is the observation space dimension, and M is the ensemble size. Then the computational complexity of EKI is $\mathcal{O}[T(M\mathcal{C}+2M\kappa n+\tau_{\max}M\mathcal{C})]$, where T is the number of tempering iterations, $\tau_{\max}$ is the number of pcn-MCMC inner iterations, and $\mathcal{C}$ is computational cost of a forward model F. For the pseudocode of the EKI method please refer to the Algorithm 5 in Appendix A.

2.5 Hybrid

Despite the underlying Gaussian assumption the EKI is remarkable robust in non-linear high-dimensional settings opposed to consistent SMC methods such as the TET(S)PF. For many non-linear problems it is desirable to have better uncertainty estimates while maintaining a level of robustness. This can be achieved by factorising the likelihood given by Eq. (2), e.g,

$$g(\boldsymbol{u};\boldsymbol{y}_{\mathrm{obs}}) = g_1(\boldsymbol{u};\boldsymbol{y}_{\mathrm{obs}})\cdot g_2(\boldsymbol{u};\boldsymbol{y}_{\mathrm{obs}}),$$

where

$$g_1(\boldsymbol{u}; \boldsymbol{y}_{\text{obs}}) = \beta g(\boldsymbol{u}; \boldsymbol{y}_{\text{obs}}) = \exp\left[-\frac{1}{2}(F(\boldsymbol{u}) - \boldsymbol{y}_{\text{obs}})'(\beta \mathbf{R})^{-1}(F(\boldsymbol{u}) - \boldsymbol{y}_{\text{obs}})\right] \tag{14}$$

230 and

$$g_2(\boldsymbol{u}; \boldsymbol{y}_{\text{obs}}) = (1-\beta)g(\boldsymbol{u}; \boldsymbol{y}_{\text{obs}}) = \exp\left[-\frac{1}{2}(F(\boldsymbol{u}) - \boldsymbol{y}_{\text{obs}})'[(1-\beta)\mathbf{R}]^{-1}(F(\boldsymbol{u}) - \boldsymbol{y}_{\text{obs}})\right]. \tag{15}$$

Then it is possible to alternate between methods with complementing properties such as the EKI and the TET(S)PF updates e.g., likelihood

$$\exp\left[-\frac{\beta}{2}(F(\boldsymbol{u}) - \boldsymbol{y}_{\text{obs}})'\mathbf{R}^{-1}(F(\boldsymbol{u}) - \boldsymbol{y}_{\text{obs}})\right]^{(\phi_t - \phi_{t-1})}$$

235 is used for an EKI update followed by an update with a TET(S)PF on the basis of

$$\exp\left[-\frac{(1-\beta)}{2}(F(\boldsymbol{u}) - \boldsymbol{y}_{\text{obs}})'\mathbf{R}^{-1}(F(\boldsymbol{u}) - \boldsymbol{y}_{\text{obs}})\right]^{(\phi_t - \phi_{t-1})}.$$

This combination of an approximative Gaussian method and a consistent SMC method has been referred to as hybrid filters in the data assimilation literature[1](Chustagulprom et al., 2016; Frei and Künsch, 2013). This ansatz can also be understood as using the EKI as an more elaborate proposal density for the importance sampling step within SMC.

240 *Computational complexity.* The computational complexity of combining the two algorithms is $\mathcal{O}[T(M\mathcal{C} + 2M\kappa n + M\mathcal{C} + M^3 \log M + \tau_{\max} M\mathcal{C})]$ for the hybrid EKI-TETPF and $\mathcal{O}[T(M\mathcal{C} + 2M\kappa n + M\mathcal{C} + M^2 C(\alpha) + \tau_{\max} M\mathcal{C})]$ for the hybrid EKI-TESPF. For the pseudocode of the hybrid methods please refer to the Algorithm 6 in Appendix A.

3 Numerical experiments

We consider a steady-state single-phase Darcy flow model defined over an aquifer of two-dimensional physical domain $D = [0,6] \times [0,6]$, which is given by

$$-\nabla \cdot [k(x,y)\nabla P(x,y)] = f(x,y), \quad (x,y) \in D, \tag{16}$$

where $\nabla = (\partial/\partial x \ \partial/\partial y)'$, $\cdot$ the dot product, $P(x,y)$ the pressure, $k(x,y)$ the permeability, and $f(x,y)$ the source term. The source term is

$$f(x,y) = \begin{cases} 0 & \text{if } 0 < y \leq 4, \\ 137 & \text{if } 4 < y < 5, \\ 274 & \text{if } 5 < y \leq 6. \end{cases} \tag{17}$$

250 The boundary conditions are

$$P(x,0) = 100, \quad \frac{\partial P}{\partial x}(6,y) = 0, \quad -k(0,y)\frac{\partial P}{\partial x}(0,y) = 500, \quad \frac{\partial P}{\partial y}(x,6) = 0, \tag{18}$$

where ∂D is the boundary of domain D.

---

[1]Note that the terminology is also used in the context of data assimilation filters combining variational and sequential approaches.
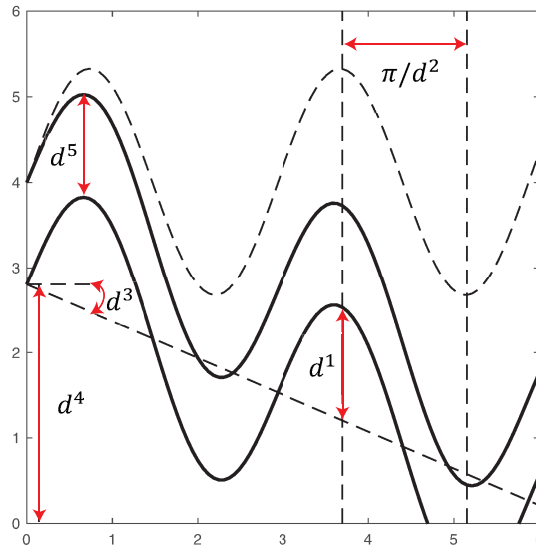
Figure 1. Geometrical configuration of channel flow: amplitude d^1, frequency d^2, angle d^3, initial point d^4, and width d^5.

3.1 Parameterisation of permeability

We consider the following two parameterisations of the permeability function $k(x,y)$

255 P1: log permeability over the entire domain D, $u(x,y) = \log k(x,y)$;

P2: permeability over domain D that has a channel, $k(x,y) = k^1(x,y)\delta_{D_c}(x,y) + k^2(x,y)\delta_{D \setminus D_c}(x,y)$ as by Iglesias et al. (2014).

Here D_c denotes a channel, δ Dirac function, $k^1 = \exp(u^1(x,y))$ and $k^2 = \exp(u^2(x,y))$ denote permeabilities inside and outside the channel. The geometry of the channel is parameterized by five parameters $\{d^i\}_{i=1}^5$: amplitude, frequency, angle,

260 initial point, and width, correspondingly. The lower boundary of the channel is given by $y = d^1 \sin(d^2 x/6) + \tan(d^3)x + d^4$. The upper boundary of the channel is given by $y + d^5$. These parameters are depicted in Fig. 1.

We assume log permeability for both P1 and P2 is drawn from a Gaussian distribution $\mu_0 = \mathcal{N}(m, C)$ with mean m and covariance C. We define C via a correlation function given by the Wittle-Matern correlation function defined by Matérn (1986)

$$c(x,y) = \frac{1}{\gamma(1)} \frac{\|x-y\|}{\upsilon} \Upsilon_1 \left(\frac{\|x-y\|}{\upsilon} \right),$$

265 where γ is the gamma function, $\upsilon = 0.5$ is the characteristic length scale, and Υ_1 is the modified Bessel function of the second kind of order 1.

We implement a cell-centered finite difference method to solve the forward model Eqs. (16)–(18) on an $N \times N$ grid. We denote by $\boldsymbol{\lambda}$ and $\mathbf{V}$ eigenvalues and eigenfunctions of the corresponding covariance matrix $\mathbf{C}$, respectively. Then, following a

Karhunen-Loeve expansion, log permeability is

$$270 \quad \log(k^l) = \log(m) + \sum_{\ell=1}^{N^2} \sqrt{\lambda^\ell} V^{\ell l} u^\ell \quad \text{for} \quad l = 1, \ldots, N^2,$$

where u^ℓ is i.i.d. from $\mathcal{N}(0,1)$ for $\ell = 1, \ldots, N^2$.

For P1, the prior for log permeability is a Gaussian distribution with mean 5. The grid dimension is 70, and thus the uncertain parameter $\boldsymbol{u} = \{u^\ell\}_{\ell=1}^{N^2}$ has dimension 4900.

For P2, we assume geometrical parameters $\boldsymbol{d} = \{d^i\}_{i=1}^5$ are drawn from uniform priors, namely $d^1 \sim U[0.3, 2.1]$, $d^2 \sim$ 275 $U[\pi/2, 6\pi]$, $d^3 \sim U[-\pi/2, \pi/2]$, $d^4 \sim U[0, 6]$, $d^5 \sim U[0.12, 4.2]$. Furthermore, we assume independence between geometric parameters and log permeability. The prior for log permeability is a Gaussian distribution with mean 15 outside the channel and with mean 100 inside the channel. The grid dimension is 50. Log permeability inside channel $\boldsymbol{u}^1 = \{u^{1,\ell}\}_{\ell=1}^{N^2}$ and log permeability outside channel $\boldsymbol{u}^2 = \{u^{2,\ell}\}_{\ell=1}^{N^2}$ are defined over the entire domain 50×50. Therefore, for P2 inference the uncertain parameter $\boldsymbol{u} = \{\boldsymbol{d}, \boldsymbol{u}^1, \boldsymbol{u}^2\}$ has dimension 5005. Moreover, for P2 we use the Metropolis-within-Gibbs methodology 280 following Iglesias et al. (2014) to separate geometrical parameters and log permeability parameters within the mutation step, since it allows to better exploit the structure of the prior.

3.2 Observations

Both the true permeability and an initial ensemble are drawn from the same prior distribution as the prior includes knowledge about geological properties. However, an initial guess is computed on a coarse grid and the true solution is computed on a fine 285 grid that has twice the resolution of the coarse grid. The synthetic observations are obtained by

$$\boldsymbol{y}_{\text{obs}} = \boldsymbol{L}(\boldsymbol{P}^{\text{true}}) + \boldsymbol{\eta}.$$

An element of $\boldsymbol{L}(\boldsymbol{P}^{\text{true}})$ is a linear functional of pressure, namely

$$L^j(\boldsymbol{P}^{\text{true}}) = \frac{1}{2\pi\sigma^2} \sum_{i=1}^{N_{\text{f}}} \exp\left(-\frac{\|\boldsymbol{X}^i - \boldsymbol{h}^j\|^2}{2\sigma^2}\right) (P^{\text{true}})^j \Delta x^2 \quad \text{for} \quad j = 1, \ldots, \kappa.$$

Here $\sigma = 0.01$, Δx^2 is the size of a grid cell $\boldsymbol{X}^i = (X^i, Y^i)$, N_{f} is resolution of a fine grid, $\boldsymbol{h}^j$ is the location of the observation 290 and κ is the number of observations. This form of the observation functional and the parameterization P1 and P2 guaranty the continuity of the forward map from the uncertain parameters to the observations and thus the existence of the posterior distribution as shown by Iglesias et al. (2014). The observation noise $\boldsymbol{\eta}$ is drawn from a normal distribution with zero mean and known covariance matrix $\mathbf{R}$. We choose the observation noise to be 2 % of L2-norm of the true pressure. Such a small noise makes the data assimilation problem hard to solve, since the likelihood is very peaked and a non-iterative data assimilation 295 approach fails.

To save computational costs, we choose ESS threshold $M_{\text{thresh}} = M/3$ for tempering, and the length of Markov chain $\tau_{\text{max}} = 20$ for mutation.

3.3 Metrics

We conduct numerical experiments with ensemble sizes 100 and 500, and 20 simulations with different initial ensemble real-
izations to check the robustness of results. We analyze the method's performance with respect to a pcn-MCMC solution from
here on referred to as reference. An MCMC solution was obtained by combining 50 independent chains each of length 10^6,
10^5 burn-in period and 10^3 thinning. For log permeability, we compute RMSE of the mean

$$\text{RMSE} = \sqrt{(\bar{\boldsymbol{u}} - \bar{\boldsymbol{u}}^{\text{ref}})'(\bar{\boldsymbol{u}} - \bar{\boldsymbol{u}}^{\text{ref}})}, \quad \text{where} \quad \bar{\boldsymbol{u}} = \frac{1}{M}\sum_{i=1}^{M}\boldsymbol{u}_i, \tag{19}$$

and $\boldsymbol{u}^{\text{ref}}$ is the reference solution.

For geometrical parameters $\boldsymbol{d}$, we compute the Kullback-Leibler divergence

$$\text{D}_{\text{KL}}^i(p^{\text{ref}} \| p) = \sum_{j=1}^{M_{\text{b}}} p^{\text{ref}}(d_j^i)\log\frac{p^{\text{ref}}(d_j^i)}{p(d_j^i)}, \tag{20}$$

where $p^{\text{ref}}(d^i)$ is the reference posterior, $p(d^i)$ is approximated by the weights, and $M_{\text{b}} = M/10$ is a chosen number of bins.

3.4 Application to P1 inference

For P1, we perform numerical experiments using 36 uniformly distributed observations, which are displayed in circles in
Fig. 3(a). We plot box plot of RMSE given by Eq. (19) over 20 independent simulations in Fig. 2(a) using Sinkhorn approxi-
mation and in Fig. 2(b) using optimal transport. The x-axis is for the hybrid parameter β, whose value 0 corresponds to EKI
and 1 to an adaptive SMC method with either Sinkhorn approximation (TESPF) or optimal transport (TETPF). Ensemble size
$M = 100$ is shown in red and $M = 500$ in green. First, we observe that at a small ensemble size 100 TESPF outperforms
TETPF. Since Sinkhorn approximation is a regularization of an optimal transport solution, TESPF provides a smoother solu-
tion than TETPF that can be seen in Fig. 3(c) and Fig. 3(f), respectively, where we plot mean log permeability. Next, we see
in Fig. 2 that the hybrid approach decreases RMSE compared to TET(S)PF: the smaller β the smaller median of RMSE. EKI
gives the smallest error due to the Gaussian parametrization of permeability. The advantage of the hybrid approach is most
pronounced at a large ensemble size 500 and optimal transport resampling.

We plot mean log permeability at ensemble size 100 and a smallest RMSE over 20 simulations in Fig. 3(b)–(f) and of
reference in Fig. 3(a). We see that EKI and TETPF(0.2) estimate well mot only large-scale feature but also small-scale feature
(e.g., negative mean at the top right corner) unlike TET(S)PF and TESPF(0.2).

3.5 Application to P2 inference

For P2, we perform numerical experiments using 9 uniformly distributed observations. which are displayed in circles in
Fig. 9(a). First, we display results obtained by Sinkhorn approximation. In Fig. 4, we plot box plot over 20 independent
runs of KL divergence given by Eq. (20) for amplitude (a), frequency (b), angle (c), initial point (d), and width (e) that define
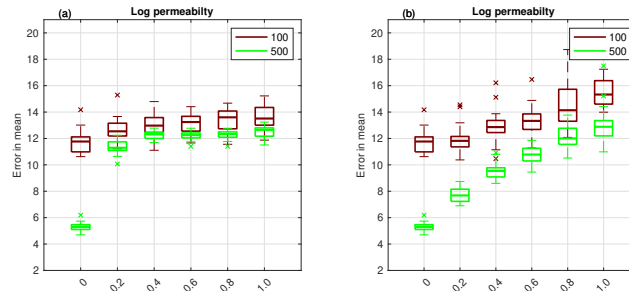
Figure 2. Application to P1 parameterization: using Sinkhorn approximation (a) and optimal transport resampling (b). Box plot over 20 independent simulations of RMSE of mean log permeability. X-axis is for the hybrid parameter, where $\beta = 0$ corresponds to EKI and $\beta = 1$ to TET(S)PF. Ensemble size 100 is shown in red, and 500 in green. Central mark is the median, edges of the box are the 25th and 75th percentiles, whiskers extend to the most extreme datapoints, and crosses are outliers.
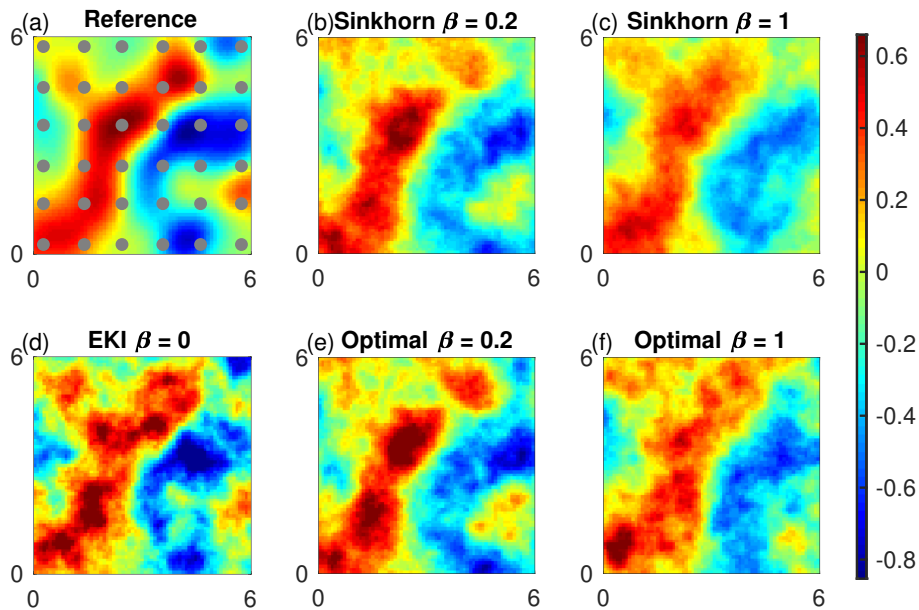

Figure 3. Mean log permeability for P1 inference for the lowest error at ensemble size 100. Observation locations are shown in circles. Reference (a), TESPF(0.2) (b), TESPF (c), EKI (d), TETPF(0.2) (e), and TETPF (f).

channel. We see that EKI outperforms any TESPF(·) including TESPF for amplitude (a) and width (e). This is due to Gaussian-like posteriors of these two geometrical parameters displayed in Fig. 6(c) and Fig. 6(o), respectively. Due to Gaussian-like posteriors the hybrid approach decreases RMSE compared to TESPF: the smaller β the smaller median of RMSE.

For frequency, angle, and initial point, whose KL divergence is displayed in Fig. 4(b), (c), and (d), respectively, the behaviour

330 of adaptive SMC is nonlinear in terms of β. This is due to non Gaussian-like posteriors of these three geometrical parameters shown in Fig. 6(f), (i), and (l), respectively. Due to non Gaussian-like posteriors the hybrid approach gives an advantage over
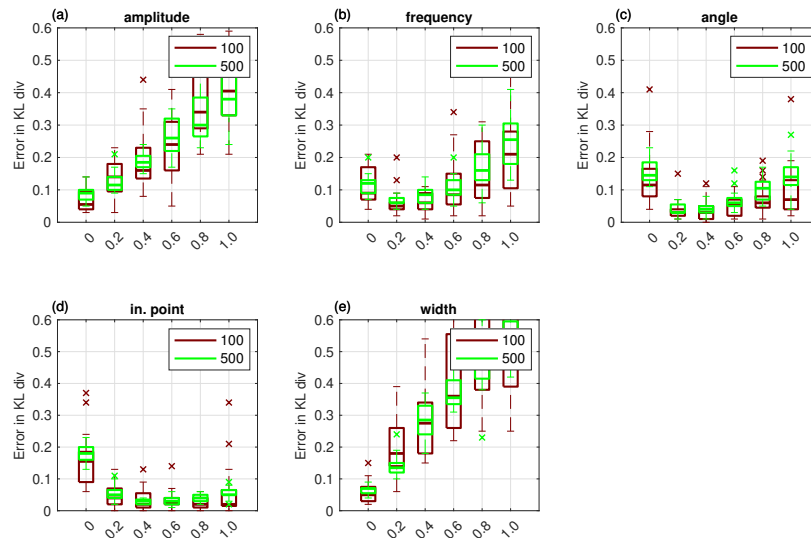
Figure 4. Application to P2 parameterization using Sinkhorn approximation. Box plot over 20 independent simulations of KL divergence for geometrical parameters: amplitude (a), frequency (b), angle (c), initial point (d), and width (e). X-axis is for the hybrid parameter, where $\beta = 0$ corresponds to EKI and $\beta = 1$ to TET(S)PF. Ensemble size 100 is shown in red, and 500 in green. Central mark is the median, edges of the box are the 25th and 75th percentiles, whiskers extend to the most extreme datapoints, and crosses are outliers.

both TESPF and EKI—there exists a $\beta \neq 0$ for which the KL divergence is lowest though it is inconsistent between geometrical parameters.

When comparing TESPF($\cdot$) to TETPF($\cdot$), we observe the same type of behaviour in terms of β: linear for amplitude and

335 width, whose KL divergence is displayed in Fig. 5(a) and (e), respectively, and nonlinear for frequency, angle, and initial point, whose KL divergence is displayed in Fig. 5(b), (c), and (d), respectively. However, the KL divergence is smaller when optimal transport resampling is used instead of Sinkhorn approximation.

In Fig. 6, we plot posterior of geometrical parameters: amplitude (a)–(c), frequency (d)–(f), angle (g)–(i), initial point (j)–(l), and width (m)–(o), where on the left TESPF(0.2), in the middle TETPF(0.2), and on the right EKI are shown. In black is the

340 reference, in red 20 simulations of ensemble size 100, in green 20 simulations of ensemble size 500. The true parameters are shown as black cross. We see that as ensemble size increases posteriors approximated by TET(S)PF converge to the reference posterior unlike EKI.

Now we investigate adaptive SMC performance for permeability estimation. First, we display results obtained by Sinkhorn approximation. We plot box plot over 20 independent simulations of RMSE given by Eq. (19) for log permeability outside

345 channel in Fig. 7(a) and inside channel in Fig. 7(b). Even though log permeability is Gaussian distributed, for a small ensemble size 100 there exists a $\beta \neq 0$ that gives lowest RMSE both outside and inside channel. As ensemble size increases, methods performance becomes equivalent.
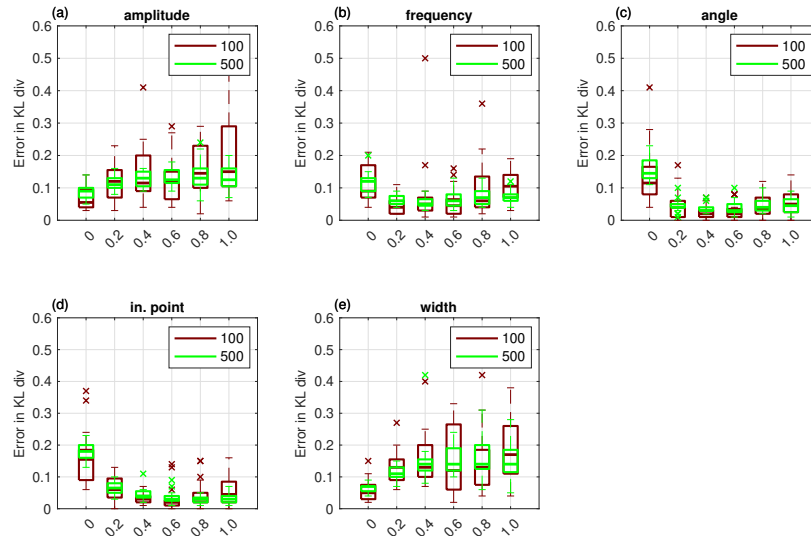
14

Figure 5. The same as Fig. 4 but using optimal transport resampling.

Next, we compare TESPF($\cdot$) to TETPF($\cdot$) for log permeability estimation outside and inside channel whose RMSE is displayed in Fig. 8(a) and (b), respectively. We observe the same type of behaviour in terms of β: nonlinear for a small ensemble

350 size 100, and equivalent for a larger ensemble size 500. Furthermore, at a small ensemble size 100 TESPF outperforms TETPF, which was also the case for P1 parameterization Sec. 3.4.

In Fig. 9, we show mean field of permeability over the channelized domain for reference for the lowest error at ensemble size 100 for TESPF(0.2) (b), TESPF (c), EKI (d), TETPF(0.2) (e), and TETPF (f). We plot mean log permeability over the channelized domain at ensemble size 100 and a smallest RMSE over 20 simulations in Fig. 9(b)–(f) and of reference in Fig. 9(a).

355 We see that TESPF(0.2) does an excellent job at such a small ensemble size by estimating well log permeability outside and inside channel, and parameters of the channel itself.

4 Conclusions

A Sinkhorn adaptation, namely the TESPF, of the previously proposed TETPF has been introduced and numerically investigated on a parameter estimation problem. The TESPF has considerable smaller computational complexity than the TETPF,

360 namely $\mathcal{O}[T(M\mathcal{C} + M^2C(\alpha) + \tau_{\max}M\mathcal{C})]$ vs $\mathcal{O}[T(M\mathcal{C} + M^3\log M + \tau_{\max}M\mathcal{C})]$, yet has similar accuracy results (see Fig. 7, 8 and 6). In particular, the TESPF outperforms the EKI for non-Gaussian distributed parameters (e.g., initial point and angle in P2). This makes the proposed method a promising option for the high dimensional nonlinear problems one is typically faced with in geophysical applications. Further, to counter balance potential robustness problems of the TETPF and its Sinkhorn adaptation a hybrid between EKI and TET(S)PF is proposed and studied by means of the two configurations of the steady-

365 state single-phase Darcy flow model. The combination of the two adaptive SMC methods with complementing properties, i.e.,
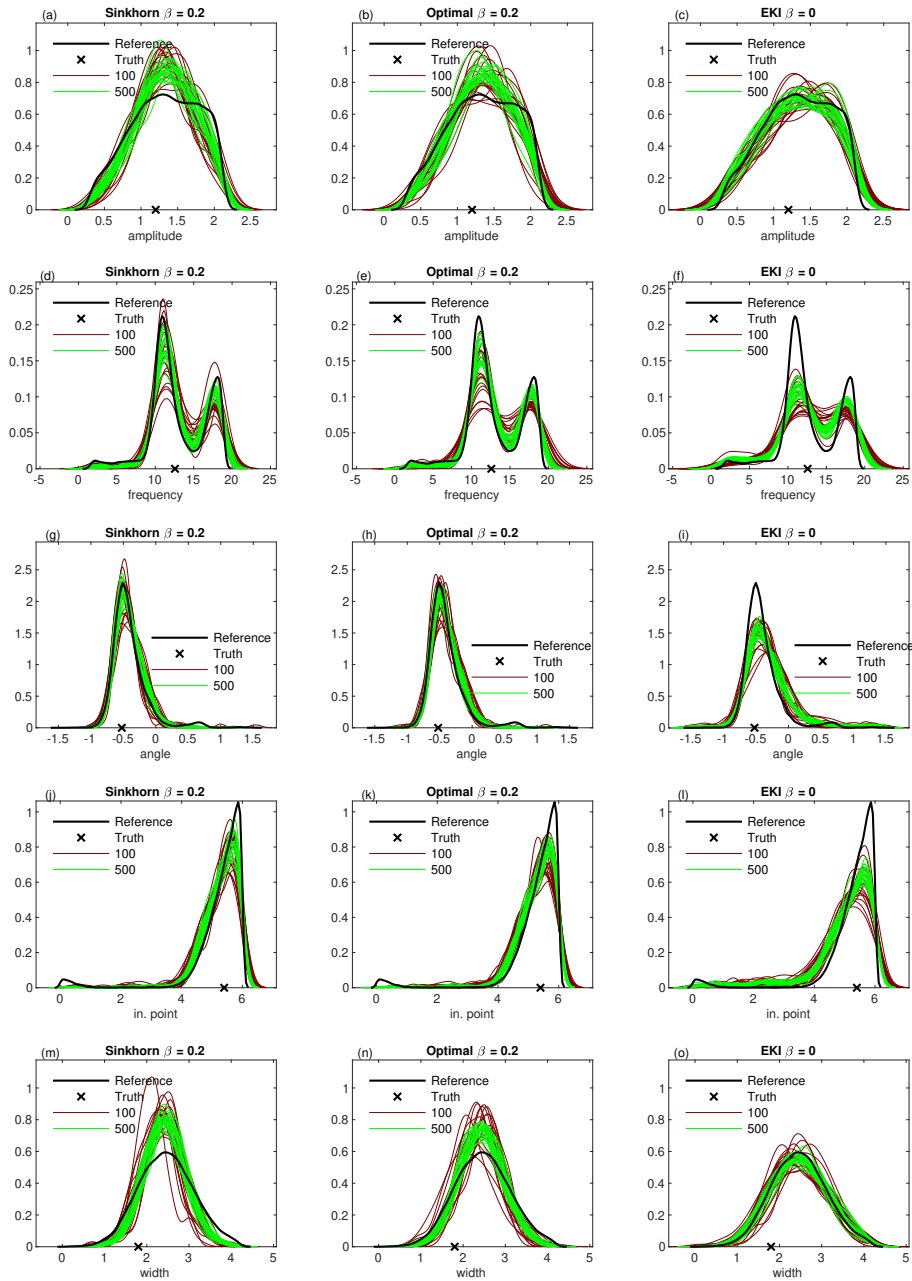
Figure 6. Posterior of geometrical parameters for P2 inference: amplitude (a)–(c), frequency (d)–(f), angle (g)–(i), initial point (j)–(l), and width (m)–(o). On the left is TESPF(0.2); in the middle is TETPF(0.2), and on the right is EKI. In black is reference, in red 20 simulations of ensemble size 100, in green 20 simulations of ensemble size 500. The true parameters are shown as black cross.

$\beta \in (0, 1)$, is superior to the individual adaptive SMC method, i.e., $\beta = 0$ or 1, for all non-Gaussian distributed parameters and performs better than the pure TETPF and the TETSPF for Gaussian distributed parameters in P1. This suggests a hybrid
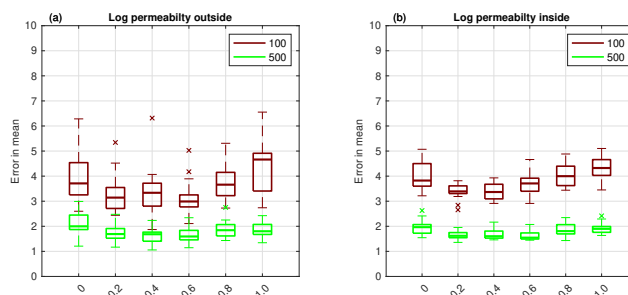
Figure 7. Application to P2 parameterization with Sinkhorn approximation. Box plot over 20 independent simulations of RMSE of mean log permeability outside channel (a) and inside channel (b). X-axis is for the hybrid parameter, where $\beta = 0$ corresponds to EKI and $\beta = 1$ to TET(S)PF. Ensemble size 100 is shown in red, and 500 in green. Central mark is the median, edges of the box are the 25th and 75th percentiles, whiskers extend to the most extreme data points, and crosses are outliers.
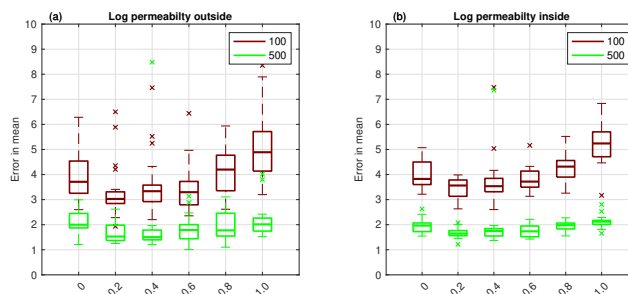

Figure 8. The same as Fig. 7 but using optimal transport resampling.

approach provides all the desirable properties required to obtain robust and highly accurate approximate solutions of nonlinear high dimensional Bayesian inference problems.
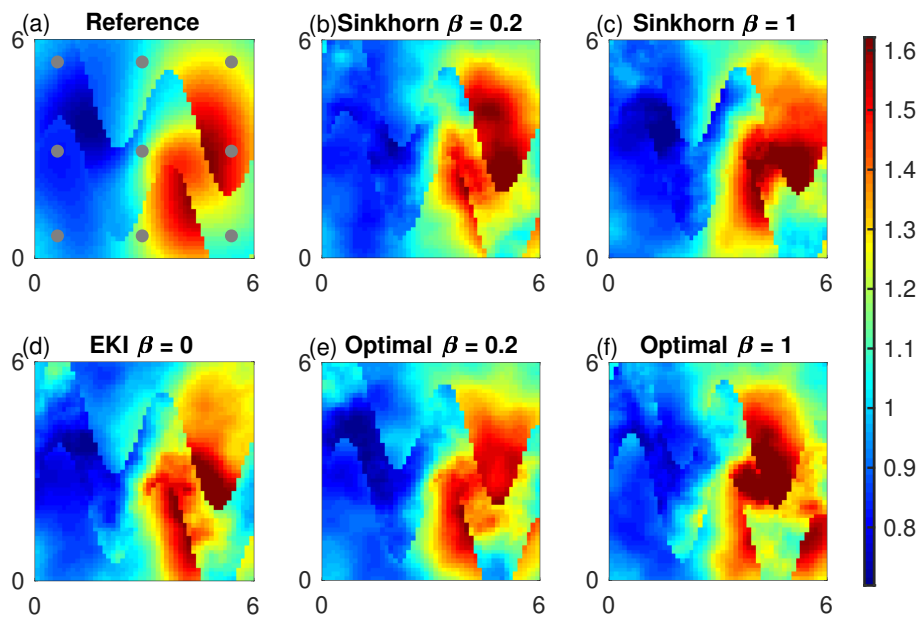
17

Figure 9. Mean log permeability for P2 inference for the lowest error at ensemble size 100. Observation locations are shown in circles. Reference (a), TESPF(0.2) (b), TESPF (c), EKI (d), TETPF(0.2) (e), and TETPF (f).

Nonlinear Processes
in Geophysics
Discussions

Open Access

EGU

370 **Appendix A: Pseudocode**

Algorithm 1 Sample mutation

Require: $\theta \in (0,1)$ and an integer $\tau_{\max}$

  for $i = 1, \ldots, M$ **do**

    Initialize $\boldsymbol{v}_i(0) = \tilde{\boldsymbol{u}}_{t,i}$

    while $\tau \le \tau_{\max}$ **do**

      Propose $\boldsymbol{v}_i^{\mathrm{prop}}$ using Eq. (5) for Gaussian probability or Eq. (6) for uniform probability

      Set $\boldsymbol{v}_i(\tau+1) = \boldsymbol{v}_i^{\mathrm{prop}}$ with probability Eq. (7) and set $\boldsymbol{v}_i(\tau+1) = \tilde{\boldsymbol{u}}_{t,i}$ with probability Eq. (8)

      $\tau \leftarrow \tau + 1$

    end while

    Set $\boldsymbol{u}_{t,i} = \boldsymbol{v}_i(\tau_{\max})$

  end for

Algorithm 2 Resampling based on optimal transport

Require: $\{\boldsymbol{u}_{t-1,i}\}_{i=1}^M$ and $\boldsymbol{w}_{t-1} = \{w_{t-1,1}, \ldots, w_{t-1,M}\}$

  Compute $\mathbf{Z}$ with $z_{ij} = \|\boldsymbol{u}_{t-1,i} - \boldsymbol{u}_{t-1,j}\|^2$

  Supply $\mathbf{Z}$ and $\boldsymbol{w}_{t-1}$ to the FastEMD algorithm of Pele & Werman with the output being the coupling $\mathbf{S}$

  Compute new samples $\{\tilde{\boldsymbol{u}}_{t,i}\}_{i=1}^M$ from Eq. (11)

Algorithm 3 Sinkhorn iteration for optimal transport problem with entropic regularisation

---

Require: regularisation parameter α, $\{\boldsymbol{u}_{t-1,i}\}_{i=1}^M$ and $\boldsymbol{w}_{t-1} = \{w_{t-1,1}, \ldots, w_{t-1,M}\}$

  Compute $\mathbf{Z}$ with $z_{ij} = \|\boldsymbol{u}_{t-1,i} - \boldsymbol{u}_{t-1,j}\|^2$

  Normalise $\mathbf{Z}$ with respect to its maximum entry

  while $\varepsilon \ge 1.0e - 8$ **do**

    $\boldsymbol{b} = \boldsymbol{w}_{t-1}./[\exp(-\alpha\mathbf{Z})\boldsymbol{a}]$

    $\boldsymbol{a} = \left(\frac{1}{M}\boldsymbol{I}_M/M\right)./[\exp(-\alpha\mathbf{Z})\boldsymbol{b}]$

    $\mathbf{S} = \mathbf{diag}(\boldsymbol{b})\exp(-\alpha\mathbf{Z})\mathbf{diag}(\boldsymbol{a})$

    $\hat{\boldsymbol{w}} = \mathbf{S}\boldsymbol{I}_M$

    $\varepsilon = \|\hat{\boldsymbol{w}} - \boldsymbol{w}_{t-1}\|$

  end while

  return $\mathbf{S}^* = \mathbf{S}$

Algorithm 4 Adaptive SMC: TET(S)PF

Require: an initial ensemble $\{\boldsymbol{u}_{0,i}\}_{i=1}^{M} \sim \mu_0$, $\theta \in (0,1)$ and integers $\tau_{\max}$ and $1 < M_{\text{thresh}} < M$

 Set $\phi_0 = 0$

 while $\phi_t \leq 1$ **do**

  $t \rightarrow t + 1$

  Compute the likelihood $g(\boldsymbol{u}_{t-1,i}; \boldsymbol{y}_{\text{obs}})$ from Eq. (2) (for $i = 1, \ldots, M$)

  Compute the tempering parameter ϕ_t:

  if $\min_{\phi \in (\phi_{t-1}, 1)} \text{ESS}_t(\phi) > M_{\text{thresh}}$ **then**

   set $\phi_t = 1$

  else

   compute ϕ_t such that $\text{ESS}_t(\phi) \approx M_{\text{thresh}}$ using a bisection algorithm on $(\phi_{t-1}, 1]$

  end if

  Compute weights $\boldsymbol{w}_{t-1} = \{w_{t-1,1}, \ldots, w_{t-1,M}\}$ from Eq. (3)

  Create new samples $\{\tilde{\boldsymbol{u}}_{t,i}\}_{i=1}^{M}$ using optimal (Sinkhorn) resampling via Algorithm 2(3)

  Compute $\{\boldsymbol{u}_{t,i}\}_{i=1}^{M}$ using sample mutation via Algorithm 1

 end while

Algorithm 5 EKI

Require: an initial ensemble $\{\boldsymbol{u}_{0,i}\}_{i=1}^{M} \sim \mu_0$, $\theta \in (0,1)$ and integers $\tau_{\max}$ and $1 < M_{\text{thresh}} < M$

 Set $\phi_0 = 0$

 while $\phi_t \leq 1$ **do**

  $t \rightarrow t + 1$

  Compute the likelihood $g(\boldsymbol{u}_{t-1,i}; \boldsymbol{y}_{\text{obs}})$ from Eq. (2) (for $i = 1, \ldots, M$)

  Compute the tempering parameter ϕ_t:

  if $\min_{\phi \in (\phi_{t-1}, 1)} \text{ESS}_t(\phi) > M_{\text{thresh}}$ **then**

   set $\phi_t = 1$

  else

   compute ϕ_t such that $\text{ESS}_t(\phi) \approx M_{\text{thresh}}$ using a bisection algorithm on $(\phi_{t-1}, 1]$

  end if

  Create new samples $\{\tilde{\boldsymbol{u}}_{t,i}\}_{i=1}^{M}$ using Eq. (13)

  Compute $\{\boldsymbol{u}_{t,i}\}_{i=1}^{M}$ using sample mutation via Algorithm 1

 end while

Algorithm 6 Hybrid EKI-TET(S)PF

Require: initial initial ensemble $\{\boldsymbol{u}_{0,i}\}_{i=1}^{M} \sim \mu_0$, $\theta \in (0,1)$, hybrid parameter β and integers $\tau_{\max}$ and $1 < M_{\text{thresh}} < M$

    Set $\phi_0 = 0$

    while $\phi_t \leq 1$ **do**

        $t \to t+1$

        Compute the likelihood $g_1(\boldsymbol{u}_{t-1,i}; \boldsymbol{y}_{\text{obs}})$ from Eq. (14) (for $i = 1, \ldots, M$)

        Set $g(\boldsymbol{u}_{t-1,i}; \boldsymbol{y}_{\text{obs}}) = g_1(\boldsymbol{u}_{t-1,i}; \boldsymbol{y}_{\text{obs}})$ (for $i = 1, \ldots, M$)

        Compute the tempering parameter ϕ_t:

        if $\min_{\phi \in (\phi_{t-1}, 1)} \text{ESS}_t(\phi) > M_{\text{thresh}}$ **then**

            set $\phi_t = 1$

        else

            compute ϕ_t such that $\text{ESS}_t(\phi) \approx M_{\text{thresh}}$ using a bisection algorithm on $(\phi_{t-1}, 1]$

        end if

        Create new samples $\{\tilde{\boldsymbol{u}}_{t,i}^{\beta}\}_{i=1}^{M}$ using Eq. (13)

        Compute the likelihood $g_2(\tilde{\boldsymbol{u}}_{t,i}^{\beta}; \boldsymbol{y}_{\text{obs}})$ from Eq. (15) (for $i = 1, \ldots, M$)

        Set $g(\boldsymbol{u}_{t-1,i}; \boldsymbol{y}_{\text{obs}}) = g_2(\tilde{\boldsymbol{u}}_{t,i}^{\beta}; \boldsymbol{y}_{\text{obs}})$ (for $i = 1, \ldots, M$)

        Compute weights $\boldsymbol{w}_{t-1} = \{w_{t-1,1}, \ldots, w_{t-1,M}\}$ from Eq. (3)

        Create new samples $\{\tilde{\boldsymbol{u}}_{t,i}\}_{i=1}^{M}$ using optimal (Sinkhorn) resampling via Algorithm 2(3)

        Compute $\{\boldsymbol{u}_{t,i}\}_{i=1}^{M}$ using sample mutation via Algorithm 1

    end while

Author contributions. S.R., S.D. and J.dW. designed the research, S.D. ran the numerical experiments, S.R., S.D. and J.dW. analyzed the results and wrote the manuscript.

Competing interests. The authors declare that they have no conflict of interest.

References

Acevedo, W., de Wiljes, J., and Reich, S.: Second-order Accurate Ensemble Transform Particle Filters, SIAM J. Sci. Comput., 39, A1834–A1850, 2017.

Agapiou, S., Papaspiliopoulos, O., Sanz-Alonso, D., and Stuart, A. M.: Importance sampling: computational complexity and intrinsic dimension, Statistical Science, 32, 405–431, https://doi.org/10.1214/17-STS611, 2017.

Beskos, A., Crisan, D., and Jasra, A.: On the stability of sequential Monte Carlo methods in high dimensions, Ann. Appl. Probab., 24, 1396–1445, https://doi.org/10.1214/13-AAP951, 2014.

Beskos, A., Jasra, A., Muzaffer, E. A., and Stuart, A. M.: Sequential Monte Carlo methods for Bayesian elliptic inverse problems, Statistics and Computing, 25, 727–737, https://doi.org/10.1007/s11222-015-9556-7, 2015.

Blömker, D., Schillings, C., Wacker, P., and Weissmann, S.: Well posedness and convergence analysis of the ensemble Kalman inversion, Inverse Problems, 35, 085 007, https://doi.org/10.1088/1361-6420/ab149c, https://doi.org/10.1088%2F1361-6420%2Fab149c, 2019.

Chustagulprom, N., Reich, S., and Reinhardt, M.: A Hybrid Ensemble Transform Particle Filter for Nonlinear and Spatially Extended Dynamical Systems, SIAM/ASA Journal on Uncertainty Quantification, 4, 592–608, https://doi.org/10.1137/15M1040967, 2016.

Cotter, S., Roberts, G., Stuart, A., and White, D.: MCMC methods for functions: modifying old algorithms to make them faster, Statistical Science, 28, 424–446, 2013.

Cuturi, M.: Sinkhorn Distances: Lightspeed Computation of Optimal Transport, in: Advances in Neural Information Processing Systems 26, edited by Burges, C. J. C., Bottou, L., Welling, M., Ghahramani, Z., and Weinberger, K. Q., pp. 2292–2300, Curran Associates, Inc., http://papers.nips.cc/paper/4927-sinkhorn-distances-lightspeed-computation-of-optimal-transport.pdf, 2013.

Dashti, M. and Stuart, A. M.: The Bayesian Approach to Inverse Problems, pp. 311–428, Springer International Publishing, Cham, https://doi.org/10.1007/978-3-319-12385-1_7, 2017.

de Wiljes, J., Pathiraja, S., and Reich, S.: Ensemble Transform Algorithms for Nonlinear Smoothing Problems, SIAM J. Sci. Comput.,, 42, A87–A114, 2020.

Del Moral, P., Doucet, A., and Jasra, A.: Sequential Monte Carlo samplers, Journal of the Royal Statistical Society: Series B (Statistical Methodology), 68, 411–436, https://doi.org/10.1111/j.1467-9868.2006.00553.x, 2006.

Ernst, O. G., Sprungk, B., and Starkloff, H.-J.: Analysis of the Ensemble and Polynomial Chaos Kalman Filters in Bayesian Inverse Problems, SIAM/ASA Journal on Uncertainty Quantification, 3, 823–851, https://doi.org/10.1137/140981319, 2015.

Evensen, G.: Analysis of iterative ensemble smoothers for solving inverse problems, Computational Geosciences, 22, 885–908, https://doi.org/10.1007/s10596-018-9731-y, 2018.

Frei, M. and Künsch, H.: Bridging the ensemble Kalman and particle filters, Biometrika, 100, 781–800, 2013.

Hairer, M., Stuart, A., and Vollmer, S.: Spectral gaps for a Metropolis–Hastings algorithm in infinite dimensions, Ann. Appl. Probab., 24, 2455–2490, 2014.

Houtekamer, P. L. and Zhang, F.: Review of the Ensemble Kalman Filter for Atmospheric Data Assimilation, Monthly Weather Review, 144, 4489–4532, https://doi.org/10.1175/MWR-D-15-0440.1, 2016.

Iglesias, M., Park, M., and Tretyakov, M.: Bayesian inversion in resin transfer molding, Inverse Problems, 34, 105 002, 2018.

Iglesias, M. A.: A regularizing iterative ensemble Kalman method for PDE-constrained inverse problems, Inverse Problems, 32, 025 002, 2016.

Iglesias, M. A., Lin, K., and Stuart, A. M.: Well-posed Bayesian geometric inverse problems arising in subsurface flow, inverse problems, 30, 114 001, 2014.

Kantorovich, L. V.: On the translocation of masses, in: Dokl. Akad. Nauk. USSR (NS), vol. 37, pp. 199–201, 1942.

Lorentzen, R. J., Bhakta, T., Grana, D., Luo, X., Valestrand, R., and Nævdal, G.: Simultaneous assimilation of production and seismic data: application to the Norne field, Computational Geosciences, 24, 907–920, https://doi.org/10.1007/s10596-019-09900-0, 2020.

Matérn, B.: Spatial Variation, Lecture Notes in Statistics, No. 36, Springer, 1986.

Monge, G.: Mémoire sur la théorie des déblais et des remblais, Histoire de l'Académie Royale des Sciences de Paris, 1781.

Neal, R. M.: Annealed importance sampling, Statistics and computing, 11, 125–139, 2001.

Pele, O. and Werman, M.: Fast and robust earth mover's distances, in: Computer vision, 2009 IEEE 12th international conference on, pp. 460–467, IEEE, 2009.

Reich, S.: A nonparametric ensemble transform method for Bayesian inference, SIAM Journal on Scientific Computing, 35, A2013–A2024, 2013.

Roberts, G. O. and Rosenthal, J. S.: Optimal scaling for various Metropolis-Hastings algorithms, Statist. Sci., 16, 351–367, https://doi.org/10.1214/ss/1015346320, 2001.

Ruchi, S., Dubinkia, S., and Iglesias, M. A.: Tempered ensemble transform particle filter for non-Gaussian elliptic problems, Inverse Problems, 35, 115 005, 2019.

Sinkhorn, R.: Diagonal equivalence to matrices with prescribed row and column sums, The American Mathematical Monthly, 74, 402–405, 1967.

Stuart, A. M.: Inverse problems: a Bayesian perspective, Acta Numerica, 19, 451–559, 2010.

Vergé, C., Dubarry, C., Del Moral, P., and Moulines, E.: On parallel implementation of sequential Monte Carlo methods: the island particle model, Statistics and Computing, 25, 243–260, https://doi.org/10.1007/s11222-013-9429-x, 2015.

Villani, C.: Optimal Transport: Old and New, Grundlehren der mathematischen Wissenschaften, Springer, 2009 edn., 2008.

Whitaker, J. S., Hamill, T. M., Wei, X., Song, Y., and Toth, Z.: Ensemble Data Assimilation with the NCEP Global Forecast System, Monthly Weather Review, 136, 463–482, https://doi.org/10.1175/2007MWR2018.1, 2008.